DOI: 10.1002/chem.200901967

Reaction Pathways Determined by Mechanical Milling Process for Dehydrogenation/Hydrogenation of the $LiNH_2/MgH_2$ System

Chu Liang, Yongfeng Liu,* Kun Luo, Bo Li, Mingxia Gao, Hongge Pan,* and Qidong Wang[a]

Abstract: The dehydrogenation/hydrogenation processes of the $LiNH_2/MgH_2$ (1:1) system were systematically investigated with respect to baller milling and the subsequent heating process. The reaction pathways for hydrogen desorption/absorption of the $LiNH_2/MgH_2$ (1:1) system were found to depend strongly on the milling duration due to the presence of two competing reactions in different stages (i.e., the reaction between $Mg(NH_2)_2$ and MgH_2 and that between $Mg(NH_2)_2$ and LiH), caused by a metathesis reaction between $LiNH_2$ and MgH_2, which exhibits more the nature of solid–solid reactions. The study provides us with a new approach for the design of novel hydrogen storage systems and the improvement of hydrogen-storage performance of the amide/hydride systems.

Keywords: amides · hydrides · hydrogen storage · reaction mechanisms · solid-state reactions

Introduction

Hydrogen is a promising alternative energy carrier. One of the key technological challenges in using hydrogen for mobile applications is the safe and efficient storage of hydrogen.[1,2] Solid-state hydrogen storage is regarded as a good solution. Numerous efforts have been made in exploring and investigating novel hydrogen-storage materials with high volumetric and gravimetric hydrogen densities during the last 10 years.[3–7] Encouraging progress was made by the introduction of nitrogen into the hydrogen storage system in 2002 when Chen et al. demonstrated that the hydrogenation of lithium nitride, Li_3N, took place reversibly with a two-step reaction [Eq. (1)]:[8]

$$Li_3N + 2H_2 \leftrightarrow Li_2NH + LiH + H_2 \leftrightarrow LiNH_2 + 2LiH \quad (1)$$

Although 11.4 wt % of hydrogen storage capacity is very attractive, the high operating temperature ($>400\,^\circ C$) for complete hydrogen desorption prevents it from practical on-board applications. An alternative approach is the partial substitution of Li with Mg, which leads to a novel Li-Mg-N-H system with improved thermodynamics. Luo and Ronnebro[9] and Xiong et al.[3] found independently that 5.5 wt % of hydrogen could be stored reversibly in $2LiNH_2/MgH_2$ and $Mg(NH_2)_2/2LiH$ systems at 180 °C with a desorption equilibrium pressure of about 20 atm by means of the following reaction [Eq. (2)]:

$$2LiNH_2 + MgH_2 \rightarrow Mg(NH_2)_2 + 2LiH \leftrightarrow Li_2MgN_2H_2 + 2H_2 \quad (2)$$

Further efforts have been devoted to the composition adjustments for obtaining higher hydrogen capacities. Leng et al. reported that the $3Mg(NH_2)_2/8LiH$ mixture absorbed/desorbed reversibly 6.9 wt % of hydrogen through the following reaction [Eq. (3)]:[10]

$$3Mg(NH_2)_2 + 8LiH \leftrightarrow 4Li_2NH + Mg_3N_2 + 8H_2 \quad (3)$$

When the molar ratio of $Mg(NH_2)_2$ to LiH was adjusted to 1:4, the hydrogen storage capacity of the mixture was increased to 9.1 wt % as shown below [Eq. (4)]:[11]

$$3Mg(NH_2)_2 + 12LiH \leftrightarrow 4Li_3N + Mg_3N_2 + 12H_2 \quad (4)$$

It is quite inspiring to see that the composition changes are able to enhance the hydrogen-storage capacity of the Li-

---

[a] C. Liang, Dr. Y. Liu, K. Luo, B. Li, Dr. M. Gao, Prof. Dr. H. Pan, Prof. Dr. Q. Wang
Department of Materials Science and Engineering
Zhejiang University, Hangzhou 310027 (China)
Fax: (+86) 571-87952615
E-mail: mselyf@zju.edu.cn
hgpan@zju.edu.cn

Supporting information for this article is available on the WWW under http://dx.doi.org/10.1002/chem.200901967.

Mg-N-H system due to the change of dehydrogenation/hydrogenation reaction pathways.

Recently, a novel $LiNH_2/MgH_2$ system with a molar ratio of 1:1 attracted our attention due to its higher hydrogen capacity and improved thermodynamics. Alapati et al. first predicted the thermodynamic feasibility of the following reaction by first-principles calculations based on density function theory (DFT) [Eq. (5)]:[12]

$$LiNH_2 + MgH_2 \rightarrow LiMgN + 2H_2 \tag{5}$$

The desorption enthalpy change calculated is $29.7\,kJ\,mol^{-1}$ of H_2 at 0 K, which is an acceptable value for on-board hydrogen-storage applications. Further first-principles calculations showed that the reaction between $LiNH_2$ and MgH_2 at a molar ratio of 1:1 might be a multistep reaction as follows [Eq. (6)]:[13]

$$\begin{aligned} LiNH_2 + MgH_2 &\rightarrow \tfrac{1}{2}Mg(NH_2)_2 + LiH + \tfrac{1}{2}MgH_2 \\ &\rightarrow LiH + \tfrac{1}{4}Mg(NH_2)_2 + \tfrac{1}{4}Mg_3N_2 + H_2 \\ &\rightarrow \tfrac{1}{2}LiH + \tfrac{1}{4}Li_2MgN_2H_2 + \tfrac{1}{4}Mg_3N_2 + \tfrac{3}{2}H_2 \\ &\rightarrow LiMgN + 2H_2 \end{aligned} \tag{6}$$

However, Osborn et al. found experimentally that the $LiNH_2/MgH_2$ (1:1) mixture milled for 3 h followed a new chemical process pathway at 210 °C near equilibrium conditions instead of the originally predicted reactions in Equations (5) and (6), as described below [Eq. (7)]:[14]

$$LiNH_2 + MgH_2 \rightarrow \tfrac{1}{3}Li_2Mg_2(NH)_3 + \tfrac{1}{3}MgH_2 + \tfrac{1}{3}LiH + H_2 \tag{7}$$

Although Lu et al. reported that approximately 8.1 wt % of hydrogen, a theoretical value of hydrogen desorption for the reaction in Equation (5), was observed by means of thermogravimetric analysis (TGA) from the sample milled for 24 h,[15] the effects of the coproduct of ammonia have not been eliminated, and hence the details of structural information of the solid products need to be further ascertained. Unlike the previous investigations, our recent work pointed out that four sequential reactions proceeded during 36 h of ball milling and the subsequent heating process for the $LiNH_2/MgH_2$ (1:1) mixture [Eq. (8)]:[16]

$$\begin{aligned} &LiNH_2 + MgH_2 \xrightarrow{\text{milled for 12h}} \tfrac{1}{2}Mg(NH_2)_2 + LiH + \tfrac{1}{2}MgH_2 \\ &\xrightarrow{\text{milled for 36h}} LiH + \tfrac{1}{4}Mg(NH_2)_2 + \tfrac{1}{2}MgNH + \tfrac{1}{4}MgH_2 + \tfrac{1}{2}H_2 \\ &\xrightarrow{\text{heated to 220°C}} \tfrac{1}{2}LiH + \tfrac{1}{4}Li_2MgN_2H_2 + \tfrac{1}{2}MgNH + \tfrac{1}{4}MgH_2 + H_2 \\ &\xrightarrow{\text{heated to 390°C}} \tfrac{1}{4}Mg_3N_2 + \tfrac{1}{4}Li_2MgN_2H_2 + \tfrac{1}{2}LiH + \tfrac{3}{2}H_2 \end{aligned} \tag{8}$$

However, it is worth mentioning here that the ternary nitride product, LiMgN, which was predicted by Akbarzadel et al.,[13] has not been obtained even though the sample was heated up to 390 °C in our experiment.

Since investigations on the ball-milled $LiNH_2$-MgH_2 (1:1) mixture by several research groups resulted in different dehydrogenation processes, we became highly motivated toward understanding the underlying mechanisms of the chemical reaction between $LiNH_2$ and MgH_2 with a molar ratio of 1:1. In this study, we have concentrated on elucidating the correlation between mechanical ball milling and the hydrogen-desorption reactions of the $LiNH_2/MgH_2$ (1:1) mixture. The conclusion that the milling duration determines the reaction pathways for hydrogen storage within this system has been elucidated in detail by a series of structural examinations associated with hydrogen-storage measurements. These facts provided us with insights into the reason for the discrepancies in the experimental results of the $LiNH_2/MgH_2$ (1:1) system reported previously by several research groups.[13–16] The furtherance of understanding of the reaction mechanism of the $LiNH_2/MgH_2$ (1:1) system in this work is expected to facilitate the design of a new amide/hydride combined system with improved hydrogen-storage properties.

Results and Discussion

Dehydrogenation reactions in the ball-milling process: In our previous work,[16] it was reported that the NH_2 group in $LiNH_2$ and the hydrogen atoms in MgH_2 first switched places with each other and then hydrogen was liberated gradually during ball milling of the $LiNH_2$ and MgH_2 (1:1) mixture, as described in the first and second steps of the reaction in Equation (8). After being milled for 36 h, around 0.9 mol of hydrogen atoms were released from 1 mol of the $LiNH_2/MgH_2$ (1:1) mixture. In this work, the milling time was purposely further prolonged to enable us to realize in depth the mechanical-milling dependence of the hydrogen-desorption reactions. It was found that more hydrogen was evolved from the $LiNH_2/MgH_2$ (1:1) mixture during the increased milling time. After 48 h of milling, the interior pressure of the milling jar was increased to 5.1 atm, equivalent to 1.5 mol of hydrogen atoms being released per unit formula of $1\,LiNH_2/1\,MgH_2$. Quite clearly, a 0.6 mol increase in hydrogen desorption was obtained compared with the sample milled for 36 h.[16] Since, during the entire span of 36 h of milling, the $LiNH_2/MgH_2$ (1:1) mixture was converted to the mixture of $0.5\,MgNH/0.25\,Mg(NH_2)_2/LiH/0.25\,MgH_2$ along with hydrogen release,[16] this result made us believe that further hydrogen desorption was possible from a continuous reaction between the remaining $Mg(NH_2)_2$ and MgH_2 [Eq. (9)]:

$$\tfrac{1}{8}Mg(NH_2)_2 + \tfrac{1}{8}MgH_2 \rightarrow \tfrac{1}{4}MgNH + \tfrac{1}{4}H_2 \tag{9}$$

To justify our inference, the structure of the solid product after 48 h of milling was characterized by means of FTIR and XRD as shown in Figure 1. Evidently, one broad absorbance centered at 3178 cm^{-1} dominates the FTIR spectrum (Figure 1a), which is located in the typical N–H vibration range of imide. Additionally, another absorbance can also be found at 3265 cm^{-1}, although it is seriously distorted and its intensity is much weaker. According to the previous reports, the absorbance at 3178 cm^{-1} was assigned to MgNH,[16] and the one at 3265 cm^{-1} belonged to $Mg(NH_2)_2$.[17] The absorbance of $Mg(NH_2)_2$ seems to move towards a lower wavenumber compared with the results obtained by Liu et al.[16] and Linde et al.,[18] perhaps due to the serious distortion and the effect of the strong broad absorbance in the vicinity, which causes the difficulty in an exact readout for the peak position of the absorbance. The very weak absorbance of $Mg(NH_2)_2$ means that the concentration in the solid residue was rather low. The results indicate that longer milling time induces the incessant consumption of the species containing an NH_2 group and the corresponding development of the species with an NH group. XRD examination shows further that there are three broad diffraction peaks at 34.9, 40.5, and 58.8° (2θ), as shown in Figure 1b. According to the report by Hu et al.,[19,20] they belonged to MgNH. Thus, the structural information obtained makes us believe that the remaining $Mg(NH_2)_2$ reacted with MgH_2 to yield H_2 and form MgNH as the milling time increases from 36 to 48 h, as expressed by the following reaction [Eq. (10)]:

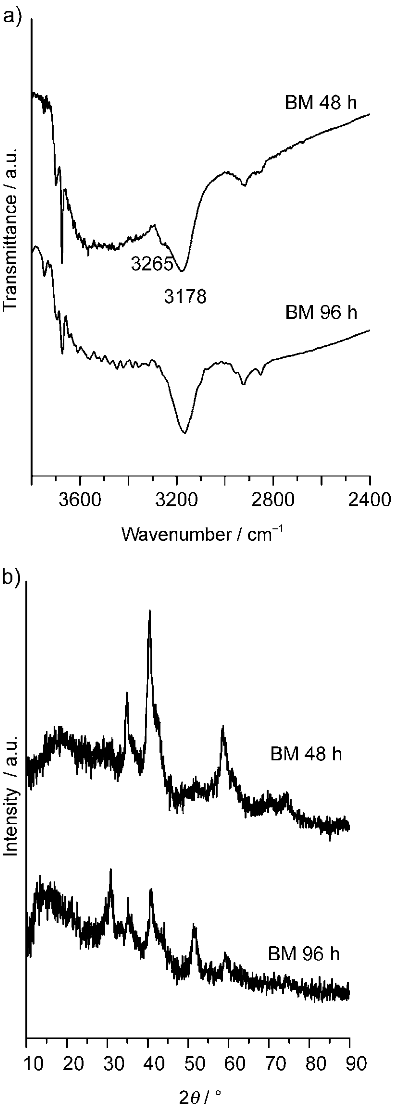

Figure 1. a) IR spectra and b) XRD patterns of the $LiNH_2/MgH_2$ (1:1) mixtures milled for 48 and 96 h.

$$\begin{aligned}&\frac{1}{2}MgNH + \frac{1}{4}Mg(NH_2)_2 + \frac{1}{4}MgH_2 + LiH \rightarrow \\ &\quad \frac{3}{4}MgNH + \frac{1}{8}Mg(NH_2)_2 + \frac{1}{8}MgH_2 + LiH + \frac{3}{4}H_2\end{aligned} \tag{10}$$

However, no further increase in hydrogen pressure was observed when the milling time was extended from 48 to 60 h, thus suggesting that the hydrogen-desorption reaction in the ball-milling process is likely to be greatly slowed down and even stopped during this period of time. This phenomenon can be attributed to two factors. One is that the reaction components were almost all consumed during the increasing milling time, and therefore the reaction rate was greatly decreased. In addition, the pressure of hydrogen desorbed inside the milling jar had increased to 5.1 atm after 48 h of milling, as mentioned above. The high hydrogen pressure possibly suppresses the reaction in Equation (9) from proceeding further. As a consequence, the interior hydrogen pressure of the milling jar stopped increasing. To demonstrate this, the interior pressure of the milling jar was reduced to absolute zero through evacuation after 48 h of milling, and then the ball milling was continued for a total of 96 h (hereafter denoted as BM 96 h). Interestingly enough, a 0.8 atm increase in pressure was detected again inside the milling jar, which corresponded to 0.25 mol of hydrogen atoms per unit formula of $LiNH_2/MgH_2$. As shown in Figure 1, structural analyses on the solid residue show that only one absorbance of the N–H vibration assignable to MgNH was observed in the FTIR spectrum along with the disappearance of that of $Mg(NH_2)_2$, and the XRD pattern of the sample is closer to that of the standard MgNH recorded in the JCPDS-ICDD database (ref. code 023-0391). Consequently, we believe that the hydrogen-desorption reaction is a continuation of that shown in Equation (9) and the final solid product should be MgNH and LiH. However, it is difficult to clearly detect LiH by means of XRD due to its low X-ray dispersion, especially after ball milling for a long time, which is also responsible for its poor visibility in the XRD profile.

On the basis of the above analyses and associated with our previous results, we would like to give a detailed picture of the chemical process of the $LiNH_2/MgH_2$ (1:1) mixture in the ball-milling process.[16] It can be described by a series of sequential reactions as follows [Eq. (11)]:

$$\begin{aligned}&\mathrm{LiNH_2 + MgH_2} \xrightarrow{\text{milled for 12h}} \tfrac{1}{2}\mathrm{Mg(NH_2)_2} + \mathrm{LiH} + \tfrac{1}{2}\mathrm{MgH_2}\\ &\xrightarrow{\text{milled for 36h}} \tfrac{1}{2}\mathrm{MgNH} + \tfrac{1}{4}\mathrm{Mg(NH_2)_2} + \mathrm{LiH} + \tfrac{1}{4}\mathrm{MgH_2} + \tfrac{1}{2}\mathrm{H_2}\\ &\xrightarrow{\text{milled for 48h}} \tfrac{3}{4}\mathrm{MgNH} + \tfrac{1}{8}\mathrm{Mg(NH_2)_2} + \mathrm{LiH} + \tfrac{1}{8}\mathrm{MgH_2} + \tfrac{3}{4}\mathrm{H_2}\\ &\xrightarrow[\text{container evacuated after 48 h of milling}]{\text{milled for 96 h}} \mathrm{MgNH + LiH + H_2}\end{aligned} \tag{11}$$

In total, two moles of hydrogen atoms can be obtained from the above reaction, which amounts to about 4.1 wt% of hydrogen. It is worth highlighting that varied milling duration results in different solid products, which will significantly affect the reaction pathways of hydrogen desorption in subsequent heating processes. To elucidate the milling time dependence of dehydrogenation reactions at elevated temperatures, the $\mathrm{LiNH_2/MgH_2}$ (1:1) mixtures that had been milled for 2, 12, 36, 48, and 96 h were subjected to hydrogen desorption/absorption measurements with increasing temperature.

Dehydrogenation performance and mechanisms in the heating process: Figure 2 shows the temperature-programmed desorption (TPD) curves of the $\mathrm{LiNH_2/MgH_2}$ (1:1) mixture milled for 2–96 h. It is apparent that the samples milled for different duration when subjected to heating processes with increased temperatures at a definite rate exhibit various dehydrogenation behaviors. The sample milled for 2 h starts to release hydrogen at around 160 °C, and the hydrogen-desorption rate speeds up gradually first and then rather sharply with increasing temperature. Unfortunately, a fair amount of ammonia was detected by an ammonia sensitive reagent ($\mathrm{Co(NO_3)_2}$ solution) when the temperature rose above 230 °C. This is believed to result from the thermal self-decomposition of $\mathrm{LiNH_2}$ due to its larger particle size and uneven mixing with $\mathrm{MgH_2}$ caused by the short milling time. With increasing milling time, the starting temperature for hydrogen desorption was dramatically depressed with a distinct reduction of ammonia emission. The starting temperatures for hydrogen desorption from the samples milled for 12 and 36 h are reduced to only around 80 and 50 °C, respectively. Moreover, two hydrogen desorption peaks are observed for the sample milled for 12 h with the peak temperatures at approximately 190 and 286 °C. It is interesting to note that the intensity of the hydrogen-desorption peak at approximately 190 °C is decreased gradually as the milling treatment proceeds further, and it becomes almost barely noticeable for the sample milled for 96 h. The fact of the variation in TPD behavior implies that the dehydrogenation process of the $\mathrm{LiNH_2/MgH_2}$ (1:1) mixture is significantly affected by the degree of mixing and hence the mechanical milling time in this experiment.

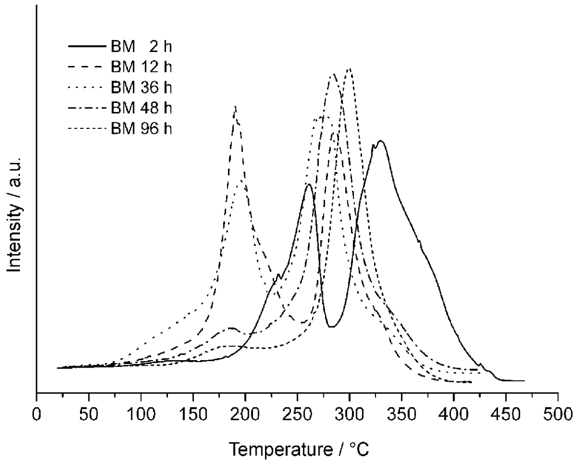

Figure 2. TPD curves of the $\mathrm{LiNH_2/MgH_2}$ (1:1) mixtures milled for 2–96 h.

The quantitative hydrogen-desorption performances of the $\mathrm{LiNH_2/MgH_2}$ mixtures with different milling duration were determined by means of volumetric method. Figure 3 shows the temperature dependence of the hydrogen-desorption amount (H/M = the gravimetric ratio of hydrogen to material) of the samples milled for 2, 12, and 48 h. For avoiding ammonia emission, the sample milled for 2 h was heated to and kept only at 210 °C for hydrogen desorption. When the temperature was held at 210 °C, the reactor was evacuated three times for more complete dehydrogenation at this temperature. Finally, approximately 3.7 wt% of hydrogen is liberated from the sample milled for 2 h, which is equivalent to 1.8 mol of hydrogen atoms per unit formula of $\mathrm{LiNH_2/MgH_2}$. This result is very close to the report by Osborn et al. on the post-3 h milled $\mathrm{LiNH_2/MgH_2}$ mixture measured by means of a pressure–composition isotherm.[14] In our experiment, newly formed $\mathrm{Li_2Mg_2N_3H_3}$ and LiH, and the remaining $\mathrm{MgH_2}$ were all detected in the dehydrogenated product by XRD and FTIR analyses as shown in Figure 4. It indicates that, during heating, in the $\mathrm{LiNH_2/MgH_2}$ mixture milled for 2 h, $\mathrm{LiNH_2}$ reacts with a due por-

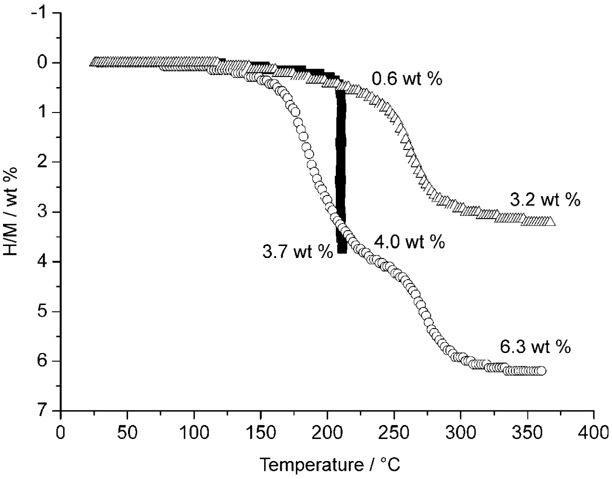

Figure 3. Quantitative hydrogen-desorption curves of the $\mathrm{LiNH_2/MgH_2}$ mixtures milled for 2 (■), 12 (○), and 48 h (△).

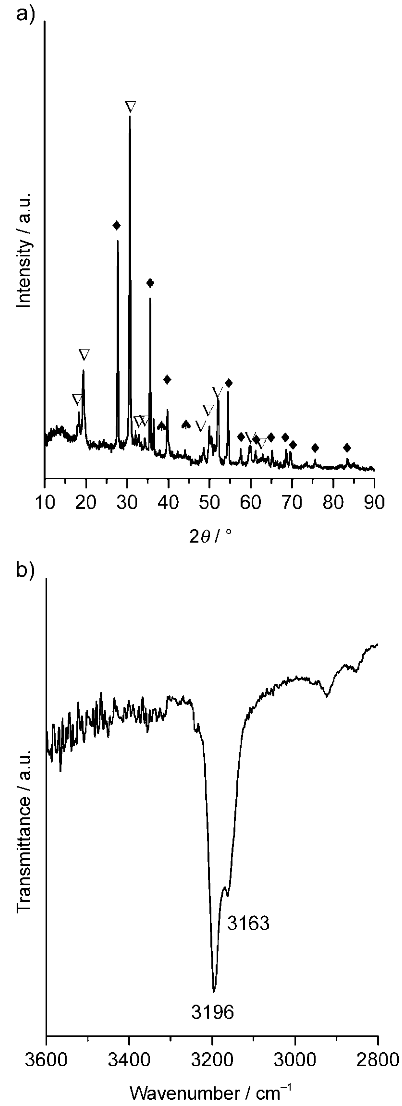

Figure 4. a) XRD pattern (▽: $Li_2Mg_2N_3H_3$, ◆: MgH_2, ♠: LiH) and b) IR spectrum of the $LiNH_2/MgH_2$ (1:1) mixture ball-milled for 2 h and then dehydrogenated at 210 °C.

tion of MgH_2 to yield H_2 and convert to $Li_2Mg_2N_3H_3$ and LiH. As a consequence, the dehydrogenation reaction of the post-2 h sample can be described by the following reaction as proposed by Osborn et al.[14] when it was heated to and kept at 210 °C [Eq. (12)]:

$$LiNH_2 + MgH_2 \rightarrow \frac{1}{3}Li_2Mg_2N_3H_3 + \frac{1}{3}LiH + \frac{1}{3}MgH_2 + H_2 \tag{12}$$

Theoretically, this reaction should be able to release approximately 4.1 wt % of hydrogen, which is close enough to the 3.7 wt % of hydrogen desorption amount measured above.

For the 12 h milling sample, an obvious two-step reaction can be identified for hydrogen desorption with a temperature change from Figure 3. The hydrogen-desorption amount is about 4.0 wt % for the first step of the reaction and 2.3 wt % for the second step, which corresponds to 2.0 and 1.1 mol of hydrogen atoms per unit formula of $LiNH_2/MgH_2$, respectively. In total, 6.3 wt % of hydrogen, equivalent to 3.1 mol of hydrogen atoms, was released from the 12 h milling sample in the temperature range of 25–360 °C. For identifying the chemical changes that occurred during the hydrogen-desorption process as the temperature increased continuously, samples at different dehydrogenation stages were collected for XRD and FTIR analyses. Figure 5 shows the XRD patterns and FTIR spectra of the samples dehydrogenated at 250 and 400 °C. We have reported that the $LiNH_2/MgH_2$ sample milled for 12 h was converted to the $0.5\,Mg(NH_2)_2/LiH/0.5\,MgH_2$ mixture.[16] After dehydrogenation at 250 °C, MgH_2 is still discernable as the dominating phase, whereas $Mg(NH_2)_2$ and LiH are not discernible in

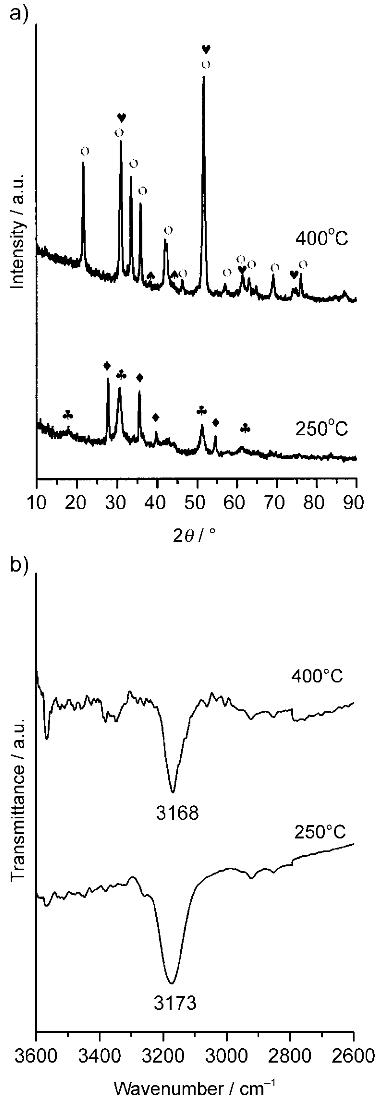

Figure 5. a) XRD patterns (◆: MgH_2, ♠: LiH, ♣: $Li_2MgN_2H_2$, ○: Mg_3N_2, ♥: Li_2NH) and b) IR spectra of the $LiNH_2/MgH_2$ (1:1) sample ball-milled for 12 h and then dehydrogenated at 250 and 400 °C.

the XRD profile (Figure 5a). A series of new diffraction peaks assignable to $Li_2MgN_2H_2$ appear at 17.9, 30.7, 51.3, and 61.3° (2θ).[21] Moreover, FTIR examination shows that only one absorbance centered at $3173\,cm^{-1}$ is found, as shown in Figure 5. This absorbance belongs to the typical N–H vibration of the imide ion in $Li_2MgN_2H_2$.[21] Hence, it can be concluded that for the sample milled for 12 h and heated up to 250 °C, $Mg(NH_2)_2$ and LiH have been consumed and the imide $Li_2MgN_2H_2$ is formed with the hydrogen released [Eq. (13)]:

$$\frac{1}{2}Mg(NH_2)_2 + LiH + \frac{1}{2}MgH_2 \rightarrow \frac{1}{2}Li_2MgN_2H_2 + \frac{1}{2}MgH_2 + H_2 \tag{13}$$

While the sample was further heated to 400 °C, the MgH_2 introduced at the start and the newly developed $Li_2MgN_2H_2$ became invisible in the XRD profile. As shown in Figure 5a, Mg_3N_2 with sharp diffraction peaks is clearly identified, and the spectra of LiH can also be detected, although its diffraction peaks are weak and distorted. In addition, one absorbance centered at $3168\,cm^{-1}$ was detected by means of FTIR; it was generated from the N–H vibration of Li_2NH as reported previously.[15,22,23] Although the main XRD diffraction peaks of Li_2NH are overlapped with those of Mg_3N_2, the increase of the relative diffraction intensity of Mg_3N_2 helps to explain the presence of Li_2NH. As described above, approximately 1.1 mol of hydrogen atoms evolved from the sample over the temperature range 250–400 °C, and the final solid product is composed mainly of Mg_3N_2 and Li_2NH. Therefore, the chemical reaction for this dehydrogenation step can be written as [Eq. (14)]:

$$\frac{1}{2}Li_2MgN_2H_2 + \frac{1}{2}MgH_2 \rightarrow \frac{1}{3}Mg_3N_2 + \frac{1}{3}Li_2NH + \frac{1}{3}LiH + \frac{2}{3}H_2 \tag{14}$$

The similar TPD behavior and identical dehydrogenation products for a dehydrogenation reaction of $Li_2MgN_2H_2$/MgH_2 (1:1) mixture (see Figure S1 in the Supporting Information) further prove the proceeding of the reaction in Equation (14) at 250–400 °C for the $LiNH_2$/MgH_2 (1:1) sample milled for 12 h.

On the basis of the above analyses, the hydrogen desorption from the sample milled for 12 h during a heating process can be described by the following reaction [Eq. (15)]:

$$\begin{aligned}&\frac{1}{2}Mg(NH_2)_2 + LiH + \frac{1}{2}MgH_2\\ &\quad\xrightarrow{\text{heated to 250°C}} \frac{1}{2}Li_2MgN_2H_2 + \frac{1}{2}MgH_2 + H_2\\ &\quad\xrightarrow{\text{heated to 400°C}} \frac{1}{3}Mg_3N_2 + \frac{1}{3}Li_2NH + \frac{1}{3}LiH + \frac{5}{3}H_2\end{aligned} \tag{15}$$

As a result, the chemical reactions that occur during the 12 h of milling and the subsequent heating process for the $LiNH_2$/MgH_2 (1:1) mixture can be summarized as follows [Eq. (16)]:

$$\begin{aligned}&LiNH_2{+}MgH_2 \xrightarrow{\text{milled for 12 h}} \frac{1}{2}Mg(NH_2)_2 + LiH + \frac{1}{2}MgH_2\\ &\quad\xrightarrow{\text{heated to 250°C}} \frac{1}{2}Li_2MgN_2H_2 + \frac{1}{2}MgH_2 + H_2\\ &\quad\xrightarrow{\text{heated to 400°C}} \frac{1}{3}Mg_3N_2 + \frac{1}{3}Li_2NH + \frac{1}{3}LiH + \frac{5}{3}H_2\end{aligned} \tag{16}$$

We have reported that the $LiNH_2$/MgH_2 mixture milled for 36 h converted to the mixture of $0.25\,Mg(NH_2)_2$/$0.5\,MgNH$/LiH/$0.25\,MgH_2$ in our previous work.[16] After dehydrogenation at 220 °C, the solid residue consisted of $Li_2MgN_2H_2$, MgNH, LiH, and MgH_2 along with 1 mol of released hydrogen atoms. As the sample was further heated to 390 °C, the resulting product was composed of Mg_3N_2, $Li_2MgN_2H_2$, and LiH. Therefore, the hydrogen desorption from the sample milled for 36 h during a heating process can be described as [Eq. (17)]:

$$\begin{aligned}&\frac{1}{2}MgNH + \frac{1}{4}Mg(NH_2)_2 + LiH + \frac{1}{4}MgH_2\\ &\xrightarrow{\text{heated to 220°C}} \frac{1}{4}Li_2MgN_2H_2 + \frac{1}{2}MgNH + \frac{1}{2}LiH + \frac{1}{4}MgH_2 + \frac{1}{2}H_2\\ &\xrightarrow{\text{heated to 390°C}} \frac{1}{4}Mg_3N_2 + \frac{1}{4}Li_2MgN_2H_2 + \frac{1}{2}LiH + H_2\end{aligned} \tag{17}$$

The overall reaction of the $LiNH_2$/MgH_2 mixture over 36 h of milling and a subsequent heating process was expressed as the following four-step reaction [Eq. (18)]:[16]

$$\begin{aligned}&LiNH_2 + MgH_2 \xrightarrow{\text{milled for 12 h}} \frac{1}{2}Mg(NH_2)_2 + LiH + \frac{1}{2}MgH_2\\ &\xrightarrow{\text{milled for 36 h}} \frac{1}{2}MgNH + \frac{1}{4}Mg(NH_2)_2 + LiH + \frac{1}{4}MgH_2 + \frac{1}{2}H_2\\ &\xrightarrow{\text{heated to 220°C}} \frac{1}{4}Li_2MgN_2H_2 + \frac{1}{2}MgNH + \frac{1}{2}LiH + \frac{1}{4}MgH_2 + H_2\\ &\xrightarrow{\text{heated to 390°C}} \frac{1}{4}Mg_3N_2 + \frac{1}{4}Li_2MgN_2H_2 + \frac{1}{2}LiH + \frac{3}{2}H_2\end{aligned} \tag{18}$$

When ball milling was prolonged to 48 h, the hydrogen-desorption versus temperature curve of the sample almost changed to a one-step reaction as shown in Figure 3. The starting temperature for hydrogen desorption is around 115 °C. Only about 0.6 wt % of hydrogen, or 0.3 molar equiv of hydrogen atoms, was released in the temperature range 115–225 °C, which corresponds to the first dehydrogenation peak of TPD of the sample milled for 48 h as shown in Figure 2. With an increase in temperature, the hydrogen-desorption amount was gradually increased. When the temperature was elevated to 400 °C, another 2.6 wt % of hydrogen, equivalent to 1.2 mol of hydrogen atoms, was desorbed. In total, around 3.2 wt % of hydrogen was evolved from the sample milled for 48 h upon heating. The XRD pattern of the dehydrogenated sample at 200 °C is found to be very similar to that of the sample milled for just 48 h, as shown in Figure 6a. The FTIR spectrum (Figure 6b) shows that only one broad absorbance can be observed, centered at 3174 cm^{-1} with a 4 cm^{-1} decrease relative to the sample right after being milled for 48 h, thereby implying that some variations have happened concerning the N–H vibration of the imide ion. Since the sample milled for 48 h is composed of 0.75 mol of MgNH, 0.125 mol of $Mg(NH_2)_2$, 1 mol of LiH, and 0.125 mol of MgH_2, we believe that the hydrogen desorption in 115–225 °C results from the reaction between $Mg(NH_2)_2$ and LiH as described by the following reaction [Eq. (19)]:

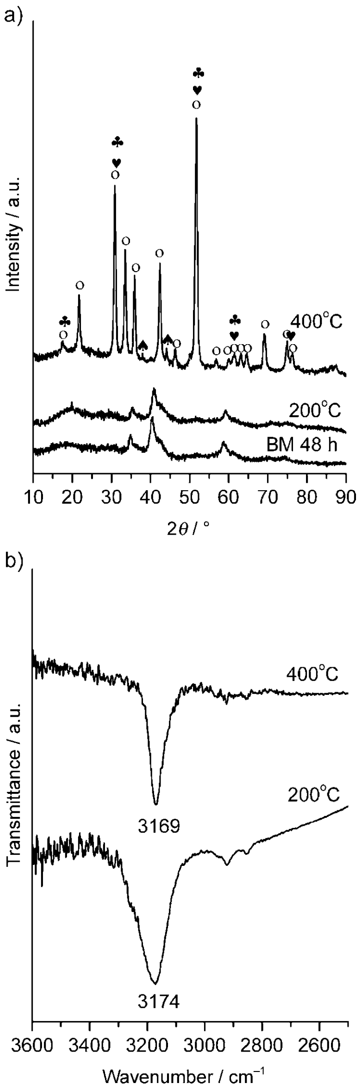

Figure 6. a) XRD patterns (○: Mg_3N_2, ♠: LiH, ♣: $Li_2MgN_2H_2$, ♥: Li_2NH) and b) IR spectra of the $LiNH_2/MgH_2$ (1:1) sample ball-milled for 48 h and then dehydrogenated at 200 and 400 °C.

$$\frac{1}{8}Mg(NH_2)_2 + \frac{1}{4}LiH \rightarrow \frac{1}{8}Li_2MgN_2H_2 + \frac{1}{4}H_2 \quad (19)$$

The amount of hydrogen actually measured is about 0.3 mol of hydrogen atoms for this step of hydrogen desorption, which is lower than the theoretical value of 0.5 mol of hydrogen atoms predicted from Equation (19). This is most likely due to the operating temperature of 225 °C being too low for the completion of the reaction of $Mg(NH_2)_2$ and LiH, as shown in Figure S2 in the Supporting Information.

For the sample dehydrogenated at 400 °C, XRD examination reveals that Mg_3N_2, LiH, and Li_2NH are all observed clearly in the dehydrogenated product, as shown in Figure 6a. At the same time, a small amount of $Li_2MgN_2H_2$ may also exist. However, it is difficult to obtain an exact readout of $Li_2MgN_2H_2$ from the XRD pattern due to the highly overlapped diffraction peaks with Mg_3N_2 and Li_2NH. FTIR spectrum measurements show one broad absorbance centered at 3169 cm^{-1} for the dehydrogenated sample at 400 °C, which is very close to the N–H vibration of the imide ion of Li_2NH (3168 cm^{-1}) as described above. Thus, the hydrogen desorption reaction in the temperature range 225–400 °C is inferred to be [Eq. (20)]:

$$\frac{3}{4}MgNH + \frac{1}{3}LiH + \frac{1}{8}MgH_2 \rightarrow \frac{7}{24}Mg_3N_2 + \frac{1}{6}Li_2NH + \frac{7}{12}H_2 \quad (20)$$

Thus, the hydrogen-desorption process can be expressed by Equation (21) as heating the sample milled for 48 h to 400 °C:

$$\begin{aligned}&\frac{3}{4}MgNH + \frac{1}{8}Mg(NH_2)_2 + LiH + \frac{1}{8}MgH_2\\&\xrightarrow{\text{heated to 225°C}} \frac{1}{8}Li_2MgN_2H_2 + \frac{3}{4}MgNH + \frac{3}{4}LiH + \frac{1}{8}MgH_2 + \frac{1}{4}H_2\\&\xrightarrow{\text{heated to 400°C}} \frac{7}{24}Mg_3N_2 + \frac{1}{8}Li_2MgN_2H_2 + \frac{1}{6}Li_2NH + \frac{5}{12}LiH + \frac{5}{6}H_2\end{aligned} \quad (21)$$

As a consequence, the hydrogen-desorption reactions of the $LiNH_2/MgH_2$ (1:1) sample milled for 48 h and subsequently subjected to a heating process to 400 °C can be summarized as follows [Eq. (22)]:

$$\begin{aligned}&LiNH_2 + MgH_2 \xrightarrow{\text{milled for 12 h}} \frac{1}{2}Mg(NH_2)_2 + LiH + \frac{1}{2}MgH_2\\&\xrightarrow{\text{milled for 48 h}} \frac{3}{4}MgNH + \frac{1}{8}Mg(NH_2)_2 + LiH + \frac{1}{8}MgH_2 + \frac{3}{4}H_2\\&\xrightarrow{\text{heated to 225°C}} \frac{1}{8}Li_2MgN_2H_2 + \frac{3}{4}MgNH + \frac{3}{4}LiH + \frac{1}{8}MgH_2 + H_2\\&\xrightarrow{\text{heated to 400°C}} \frac{7}{24}Mg_3N_2 + \frac{1}{8}Li_2MgN_2H_2 + \frac{1}{6}Li_2NH + \frac{5}{12}LiH + \frac{19}{12}H_2\end{aligned} \quad (22)$$

The hydrogen release from this reaction amounts to approximately 6.5 wt %, which is in good agreement with the experimental value of 6.3 wt %.

Apparently, the hydrogen desorption of the $LiNH_2/MgH_2$ (1:1) mixture is a complex process. Different time spent on ball milling results in different solid products with different amounts of released hydrogen, and also significantly determines the dehydrogenation reaction pathways and the quantity of hydrogen desorbed in the subsequent heating process. It is known that the initial ball milling (0–12 h) induces a metathesis reaction between $LiNH_2$ and MgH_2 to yield $Mg(NH_2)_2$ and LiH without hydrogen evolution.[16] In other words, the starting 1:1 molar ratio of the $LiNH_2$ and MgH_2 mixture was converted to the mixture of $0.5 Mg(NH_2)_2/LiH/0.5 MgH_2$ after being milled for 12 h in the present study. The reaction of $Mg(NH_2)_2$ with MgH_2 was reported to be thermodynamically favorable yet kinetically poor.[19] During ball milling, the combination of the reduced particle size, the close contact of reactants, and the high colliding energy initialize the reaction between $Mg(NH_2)_2$ and MgH_2. As a result, $Mg(NH_2)_2$ reacts with MgH_2 to release hydrogen and form MgNH as the ball milling proceeds. On the contrary, the reaction of $Mg(NH_2)_2$ with LiH is mildly endothermic with an enthalpy change of around 39 $kJ mol^{-1}$ of H_2,[24] which determines that only a very small amount of hydrogen can be released simply by ball milling, as reported previously.[21] During the heating process, however, the post-milled $Mg(NH_2)_2$ starts to react readily with LiH to generate a large amount of hydrogen and the solid residue $Li_2MgN_2H_2$ below 250 °C (see Figure S2 in the Supporting Information). From this study, we believe finally that for the $LiNH_2/MgH_2$ (1:1) system, the presence of two competing reactions in different stages including ball milling and subsequent heating is responsible for its various reaction pathways for hydrogen desorption.

Rehydrogenation performance and mechanisms: Reversibility of hydrogen storage is very important for practical applications of a hydrogen-storage system. For an understanding of the effects of the milling time on the hydrogen-absorption capability of the $LiNH_2/MgH_2$ mixture, the samples milled for 2, 12, and 48 h were first dehydrogenated completely at 210 and 360 °C, respectively, as shown in Figure 3. Then the dehydrogenated samples were subjected to hydrogen recharging under an initial 105 atm hydrogen pressure with the temperature being increased from room temperature to 210 °C. Figure 7 shows the hydrogen-absorption curves of the dehydrogenated samples milled for 2, 12, and 48 h. It is seen that the hydrogenation behavior is quite different for the samples with different milling duration. On the one hand, the onset temperature for hydrogen absorption of the samples milled for longer duration is distinctly lower than those milled for shorter duration. After dehydrogenation, the sample milled for 2 h starts to absorb hydrogen at about 160 °C, whereas the starting hydrogenation temperature of the sample milled for 12 h is only about 100 °C. This phenomenon can possibly be attributed to two factors. As described above, the $LiNH_2/MgH_2$ samples milled for 2, 12, and 48 h were converted to the mixtures of $Li_2Mg_2N_3H_3/LiH/MgH_2$, $Mg_3N_2/Li_2NH/LiH$, and $Mg_3N_2/Li_2NH/Li_2MgN_2H_2/LiH$, respectively. Different starting chemicals for hydrogen uptake should be one reason for the difference in temperatures. At the same time, the longer milling treatment leads to the reduction in particle size of the reactants, which also lowers the operating temperature of hydrogenation.[7] On the other hand, the amount of hydrogen absorbed varies with the milling duration. In the case of our experiment, when the temperature was gradually elevated to and kept at 210 °C, the hydrogen uptake amounts to 1.4, 2.7, and 2.5 wt %, which is equivalent to 0.7, 1.3, and 1.2 mol of hydrogen atoms for the samples milled for 2, 12, and 48 h, respectively. Moreover, the dehydrogenated sample milled for 36 h absorbed approximately 2.3 wt % hydrogen, as reported in our previous work.[16] These results indicate that the samples dehydrogenated differently resulted in the different hydrogen-uptake capacities. In addition, it should be noted that the hydrogen-absorption amounts for all samples are lower than that of hydrogen desorbed during their previous dehydrogenation process, thereby implying that the dehydrogenated samples have not been completely reverted to their starting states under the present testing conditions.

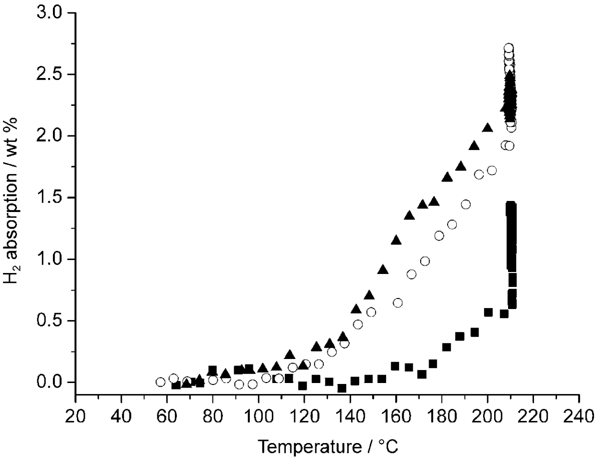

Figure 7. Hydrogen-absorption versus temperature curves of the dehydrogenated $LiNH_2/MgH_2$ samples milled for 2 (■), 12 (○), and 48 h (▲) under 105 atm hydrogen pressure.

For a deeper understanding of the reaction process that occurs during hydrogen absorption, the structures of the hydrogenated samples were characterized by means of XRD. Figure 8 shows the XRD patterns of the hydrogenated samples with different milling duration. For the sample milled for 2 h, $Mg(NH_2)_2$ can be unambiguously identified from the diffraction peaks at 14.6, 23.1, 30.1, 38.1, and 50.5° (2θ) in addition to the peaks for $Li_2Mg_2N_3H_3$, MgH_2, and LiH after hydrogenation. From the composition of the dehydrogenated sample, we believe that $Mg(NH_2)_2$ was produced during the hydrogenation of $Li_2Mg_2N_3H_3$. Xiong et al.[25] reported that $Li_2Mg_2N_3H_3$ took up some 0.5 wt % of hydrogen at 70–210 °C, which was lower than ours in the present work, probably due to the different hydrogen pressures used in two experiments. Further investigations of the hydrogen-storage properties and mechanisms of $Li_2Mg_2N_3H_3$ are in progress in our laboratory, and the results will be reported in another paper.

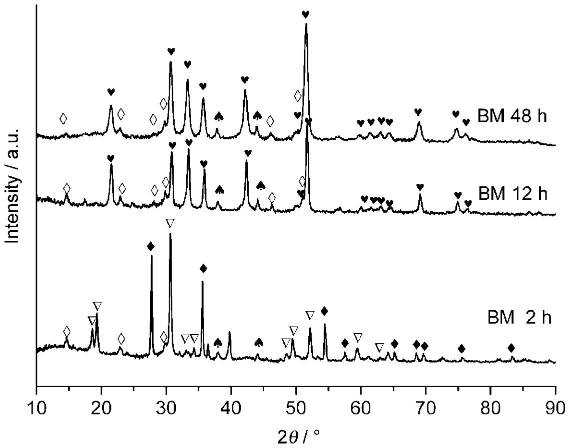

Figure 8. XRD patterns of the rehydrogenated $LiNH_2/MgH_2$ samples (♥: Mg_3N_2, ◇: $Mg(NH_2)_2$, ▽: $Li_2Mg_2N_3H_3$, ♠:LiH, ◆: MgH_2).

In the case of milling for 12 h, two phases, namely, Mg_3N_2 and LiH, dominate in the XRD profile (shown in Figure 8) after rehydrogenation. $Mg(NH_2)_2$ with weaker intensities can also be detected along with the total disappearance of Li_2NH. Leng et al. reported that the Li_2NH/Mg_3N_2 mixture with a molar ratio of 4:1 could absorb a large amount of hydrogen to form $Mg(NH_2)_2$ and LiH by the following reaction [Eq. (23)]:[10]

$$4Li_2NH + Mg_3N_2 + 8H_2 \rightarrow 3Mg(NH_2)_2 + 8LiH \quad (23)$$

As described above, for the sample milled for 12 h after dehydrogenation there were $\frac{1}{3}$ mol of Li_2NH, $\frac{1}{3}$ mol of Mg_3N_2, and $\frac{1}{3}$ mol of LiH left in the sample. The hydrogenation reaction of the dehydrogenated sample can therefore be expressed as [Eq. (24)]:

$$\frac{1}{3}Li_2NH + \frac{1}{12}Mg_3N_2 + \frac{2}{3}H_2 \rightarrow \frac{1}{4}Mg(NH_2)_2 + \frac{2}{3}LiH \quad (24)$$

Theoretically, around 1.3 mol of hydrogen atoms can be recharged in this reaction; this matches well with the experimental value mentioned above.

As for the sample milled for 36 h, the following reaction was proposed for its hydrogen-absorption process in one of our previous works [Eq. (25)]:[16]

$$\frac{1}{4}Li_2MgN_2H_2 + \frac{1}{2}H_2 \rightarrow \frac{1}{4}Mg(NH_2)_2 + \frac{1}{2}LiH \quad (25)$$

For the sample milled for 48 h, it is noted that the XRD pattern of the hydrogenated product is identical to those of the samples milled for 12 and 36 h[16] (i.e., all being composed of Mg_3N_2, $Mg(NH_2)_2$, and LiH). Since the dehydrogenated sample milled for 48 h consists of Mg_3N_2, Li_2NH, $Li_2MgN_2H_2$, and LiH, we believe that both the reactions in Equations (24) and (25) are responsible for hydrogen absorption. Taking into account the quantities of Li_2NH, $Li_2MgN_2H_2$, and Mg_3N_2 in the sample, the overall hydrogenation reaction can be written as [Eq. (26)]:

$$\begin{aligned}\frac{1}{6}Li_2NH + \frac{1}{24}Mg_3N_2 + \frac{1}{8}Li_2MgN_2H_2 + \frac{7}{12}H_2 \rightarrow \\ \frac{1}{4}Mg(NH_2)_2 + \frac{7}{12}LiH\end{aligned} \quad (26)$$

It appears that the hydrogenation-reaction pathways and the hydrogen-absorption amount of the $LiNH_2/MgH_2$ (1:1) mixture depend strongly on the component of dehydrogenated product determined by the ball-milling time. In other words, the duration of the ball-milling process determines the hydrogen-absorption process and its hydrogen-storage properties. Hence it is believed that an optimal hydrogen-storage process can be achieved for the $LiNH_2/MgH_2$ (1:1) mixture by varying ball-milling times. This approach also suggests a promising way for implementing novel hydrogen-storage systems and the improvement of existing hydrogen-storage systems. Moreover, for the basics of the process, the fact that the reaction pathways for dehydrogenation/rehydrogenation are determined by the ball-milling process speaks more to a solid–solid reaction. This developed understanding of the hydrogen-desorption reaction mechanism should be helpful in guiding the enhancement of the dehydrogenation kinetics of the amide/hydride system by catalyst loading and the reduction of particle size.

Conclusion

The hydrogen desorption/absorption properties and mechanism of the $LiNH_2/MgH_2$ (1:1) system with different ball-milling duration were systematically investigated by a series of volumetric measurements for hydrogen desorption/absorption and structural analyses (XRD and FTIR). The results showed that the reaction pathways for dehydrogenation/hydrogenation of the $LiNH_2/MgH_2$ (1:1) system depended strongly on the milling duration due to the presence of two competing reactions in different stages. The binary $1LiNH_2/1MgH_2$ mixture was first converted to the ternary $0.5Mg(NH_2)_2/LiH/0.5MgH_2$ system in the initial ball-milling stage. With prolonged ball milling, the newly developed $Mg(NH_2)_2$ reacted readily with MgH_2 to yield MgNH and evolve hydrogen. However, $Mg(NH_2)_2$ preferred to react with LiH rather than MgH_2 at elevated temperatures. The ball-milling duration dependence of reaction pathways for the $LiNH_2/MgH_2$ system implies that the hydrogen desorption should be of a solid–solid reaction nature. This developed understanding of the hydrogen-desorption reaction mechanism will significantly guide the work on the enhancement of the dehydrogenation kinetics of the amide/hydride system by the proper use of catalysts and the nanoparticles.

Experimental Section

The starting chemicals, lithium amide ($LiNH_2$) with 95 % purity and magnesium hydride (MgH_2) with 98 % purity, were purchased from Alfa Aesar and used as received without any further purification. The $LiNH_2$/MgH_2 mixtures were prepared by ball milling the corresponding chemicals in the molar ratio of 1:1 for different periods. In a typical procedure, $LiNH_2$ (approximately 1.15 g) and MgH_2 (1.3 g) were weighed and loaded into a milling jar (180 mL) in a glove box (MBRAUN) filled with pure argon to prevent the chemicals from air and moisture contamination. A gas valve that could be connected to a pressure gauge for measuring the inside pressure was mounted on the milling jar. The ball-to-sample weight ratio was about 60:1. The milling was carried out on a planetary ball mill rotating at 500 rpm for 2–96 h.

A homemade temperature-programmed desorption (TPD) system was employed to measure the gas-desorption behaviors of the $LiNH_2$/MgH_2 (1:1) samples milled for different periods. The TPD system was composed of a stainless steel microreactor and a gas chromatograph. Pure argon was used as the carrier gas. For each test, about 50 mg of sample was heated from room temperature to 460 °C at a heating rate of $2\,^{\circ}C\,min^{-1}$.

The quantitative hydrogen-storage performances of the $LiNH_2$/MgH_2 (1:1) samples after being milled were determined by the volumetric method using a homemade Sieverts-type apparatus. Precise pressure measurement and temperature control were accomplished by using high-precision pressure transducers and a temperature controller. For a typical test, each time approximately 200 mg of the sample was loaded in the glove box and into a stainless steel reactor with a thermocouple stuck into the sample interior for temperature measurement. The reactor was then connected to a homemade Sieverts apparatus. In the hydrogen-desorption experiment, the sample was heated gradually from room temperature to the desired temperature at a constant rate of $2\,^{\circ}C\,min^{-1}$ after being outgassed to a vacuum system. For hydrogen-absorption measurements, the reactor was first filled with hydrogen at 105 atm after being evacuated at room temperature, and then heated gradually up to 210 °C at a ramping rate of $1\,^{\circ}C\,min^{-1}$. The interior pressure and temperature of the reactor were automatically monitored and recorded. According to the pressures and temperatures, the quantities of hydrogen absorbed and desorbed were calculated by using the ideal gas law.

Crystal structures of the as-prepared and dehydrogenated/rehydrogenated samples were characterized by a X′Pert Pro X-ray diffractometer with $Cu_{K\alpha}$ radiation at 40 kV and 40 mA. Data were collected at room temperature with a step size of 0.05° from 10 to 90° (2θ). A homemade container was used to prevent powder samples from contacting air and moisture. N–H vibrations in the samples were identified using a Bruker Vector 22 Fourier infrared spectrometer (FTIR, Germany). The powder sample was mixed uniformly with KBr powder at a weight ratio of about 1:30 and then the mixture was cold pressed into a pellet of 13 mm diameter for testing. The transmission mode was adopted with a resolution of $4\,cm^{-1}$. Thirty-two scans were run and accumulated.

Acknowledgements

The authors would like to acknowledge financial support from the Natural Science Foundation of China (NSFC; grant nos. 50631020 and 50701040), MOST programs (grant nos. 2009AA05Z106 and 2010CB631304), Qianjiang Talent Project of Zhejiang Province (grant no. QJD0702005) and SRF for ROCS, SEM.

---

[1] L. Schlapbach, A. Züttle, *Nature* **2001**, *414*, 353–358.
[2] W. Grochala, P. P. Edwards, *Chem. Rev.* **2004**, *104*, 1283–1315.
[3] Z. Xiong, G. Wu, J. Hu, P. Chen, *Adv. Mater.* **2004**, *16*, 1522–1525.
[4] W. Luo, *J. Alloys Compd.* **2004**, *381*, 284–287.
[5] J. Lu, Z. Z. Fang, *J. Phys. Chem. B* **2005**, *109*, 20830–20834.
[6] L. Xie, J. Zheng, Y. Liu, X. Li, *Chem. Mater.* **2008**, *20*, 282–286.
[7] Y. Liu, K. Zhong, K. Luo, M. Gao, H. Pan, Q. Wang, *J. Am. Chem. Soc.* **2009**, *131*, 1862–1870.
[8] P. Chen, Z. Xiong, J. Luo, J. Lin, K. Tan, *Nature* **2002**, *420*, 302–304.
[9] W. Luo, E. Ronnebro, *J. Alloys Compd.* **2005**, *404–406*, 392–395.
[10] H. Y. Leng, T. Ichikawa, S. Hino, N. Hanada, S. Isobe, H. Fujii, *J. Phys. Chem. B* **2004**, *108*, 8763–8765.
[11] Y. Nakamori, G. Kitahara, K. Miwa, S. Towata, S. Orimo, *Appl. Phys. A* **2005**, *80*, 1–3.
[12] S. V. Alapati, J. K. Johnson, D. S. Sholl, *J. Phys. Chem. B* **2006**, *110*, 8769–8776.
[13] A. R. Akbarzadeh, V. Ozolins, C. Wolverton, *Adv. Mater.* **2007**, *19*, 3233–3239.
[14] W. Osborn, T. Markmaitree, L. L. Shaw, *J. Power Sources* **2007**, *172*, 376–378.
[15] J. Lu, Z. Z. Fang, Y. J. Choi, H. Y. Sohn, *J. Phys. Chem. C* **2007**, *111*, 12129–12134.
[16] Y. Liu, K. Zhong, M. Gao, J. Wang, H. Pan, Q. Wang, *Chem. Mater.* **2008**, *20*, 3521–3527.
[17] W. Lohstroh, M. Fichtner, *J. Alloys Compd.* **2007**, *446–447*, 332–335.
[18] V. G. Linde, R. Juza, *Z. Anorg. Allg. Chem.* **1974**, *409*, 199–214.
[19] J. Hu, G. Wu, Y. Liu, Z. Xiong, P. Chen, K. Murata, K. Sakata, G. Wolf, *J. Phys. Chem. B* **2006**, *110*, 14688–14692.
[20] J. Hu, Z. Xiong, G. Wu, P. Chen, K. Murata, K. Sakata, *J. Power Sources* **2006**, *159*, 120–125.
[21] Y. Liu, J. Hu, Z. Xiong, G. Wu, *J. Mater. Res.* **2007**, *22*, 1339–1345.
[22] Y. Kojima, Y. Kawai, *J. Alloys Compd.* **2005**, *395*, 236–239.
[23] W. Luo, S. Sickafoose, *J. Alloys Compd.* **2006**, *407*, 274–281.
[24] Z. Xiong, J. Hu, G. Wu, P. Chen, W. Luo, K. Gross, J. Wang, *J. Alloys Compd.* **2005**, *398*, 235–239.
[25] Z. Xiong, G. Wu, J. Hu, P. Chen, W. Luo, J. Wang, *J. Alloys Compd.* **2006**, *417*, 190–194.

Received: July 16, 2009